

Computational and Experimental Characterization of Natural Compounds as Therapeutic Modulators of GFAT-1 in Diabetes

Iswarya Obilineni¹, Vadivelan Ramachandran*¹, Srikanth Jupudi²

^{1,1*} Department of Pharmacology, JSS College of Pharmacy, JSS Academy of Higher Education and Research, Ooty, Nilgris, Tamil Nadu, India.

²Department of Pharmaceutical Chemistry, JSS College of Pharmacy, JSS Academy of Higher Education and Research, Ooty, Nilgris, Tamil Nadu, India.

Corresponding Author

Dr. Vadivelan Ramachandran

Professor and Head,

Department of Pharmacology,

JSS College of Pharmacy, Ooty

Abstract

Background: Glucosamine-6-phosphate synthase catalyzes the critical step of hexosamine biosynthesis pathway, results production of UDP-N-acetylglucosamine, a key metabolite that modifies protein expression causing insulin resistance. This makes GFAT a promising target for diabetes.

Methods: In this study, initially a structure-based virtual screening was done for 4,07,270 natural compounds from the COCONUT database using Schrödinger Suite 2024-2. 15 compounds were filtered based on their docking scores, binding free energy calculations and molecular dynamic simulations. A series of docking Glide docking protocol (SP and XP) followed by binding energy (MMGB/SA) calculations was performed. Later on, Cytotoxicity assays were performed using L-6 and 3T3-L1 cell lines. addition to that, glucose uptake assay was also performed.

Results: Among 4,07,270 compounds, **compound 2542** (glide g score: -10.09 kcal/mol and MMGB/SA ΔG Bind: -93.01 kcal/mol) and **compound 4636** (glide g score: -10.05 kcal/mol and MMGB/SA ΔG Bind: -90.65 kcal/mol) through high throughput virtual screening protocol. From 100ns molecular dynamics simulation it was concluded that compound 2542 was stabilized in the binding site of GFAT1 with minimal RMSD fluctuations. The **compound 2542** formed hydrogen bonding and hydrophobic interactions with various interface amino acid residues between the two domains with further substantial pharmacological justification needed to validate these molecules as GFAT 1 inhibitors. Cytotoxicity assays on L-6 and 3T3-L1 cell lines demonstrated IC₅₀ values of 50.58 and 35.20 $\mu\text{g/mL}$, respectively and Glucose uptake assay revealed a significant increase in glucose utilization with Biochanin A treatment.

Conclusion: These findings suggest that Biochanin A can inhibit Glucosamine-6-phosphate synthase enzyme and serve as potential lead for the development of novel antidiabetic agents.

Keywords: Glucosamine-6-phosphate synthase, Glutamine: D-fructose-6-phosphate amidotransferase (GFAT), hexosamine biosynthesis pathway, glucose uptake assay, Cytotoxicity assay, virtual screening, molecular dynamic simulations.

1. Introduction

Glucosamine-6-phosphate synthase¹ also called as L-Glutamine: D-fructose-6-phosphate amidotransferase (GFAT) belongs to nucleophile hydrolase family, contains penicillin acylase, aspartyl glucosaminidase and glutamine amidotransferases². Glucosamine-6-phosphate synthase contains two domains namely N-terminal domain and C-terminal isomerase domain³, each having one active centre. Glucosamine-6P synthase (GlmS) takes part in the hexosamine biosynthesis pathway resulting generation of Uridine diphosphate-*N*-acetyl glucosamine. This metabolite modulates the expression of proteins⁴ responsible for insulin resistance. On the other side, metabolites obtained from the hexosamine biosynthesis pathway serves as components of bacterial, fungal and other microbial cellwall⁵. Hence, this enzyme can be derived as an alternative drug candidate to reduce blood sugar levels and infectitious diseases⁶.

Diabetes mellitus is an illness characterized by elevated blood glucose levels often associated with disturbances in protein and fat metabolism⁷. Diabetes ranks highly as a threat to human health and global economies⁸. Yet, diabetes (predominantly type 2 diabetes), with other diseases like cardiovascular diseases has identified as major health concern of the 21st century⁹. Approximately it is evaluated that mostly occurs due to development of Type 2 diabetes¹⁰.

2. Methodology

2.1 In silico Virtual screening

Human Glucosamine-6-phosphate synthase enzyme 3D crystal structure and Glucose-6-Phosphate (6R4F.pdb) complex was selected for protein preparation using Protein preparation wizard Schrödinger 2024-3. Addition of hydrogen atoms was done and bond orders were given after removing water molecules. Missing side chains were added using PRIME module of Schrödinger 2024-3 PRIME module was used to add the side chains that were missed. Finally, the system was minimized with OPLS4 force field¹¹. Grid box was generated in linker site center by keeping the vander Waal radius scaling factor at 1.0 with 0.25 cutoff partial charges. COCONUT database [<https://coconut.naturalproducts.net/>] comprising of approximately 4 lakh natural molecules was downloaded and subjected to Virtual Screening Workflow of Schrödinger 2024-3. Prior to ligand preparation the database was subjected to prefilter options by running Qikprop and removing ligands with reactive functional groups. Ligand preparation was done by removing duplicate structures, adding hydrogen atoms, generating tautomers followed by optimization of ligand structures at pH 7±2. The obtained low energy conformers were flexibly docked into the generated grid box of 6R4F.pdb through a series of docking protocol. A Glide HTVS, Standard and Extra Precision docking were performed having top 10% compounds after each docking step with default parameters¹²

2.2 Post docking minimization (MMGB-SA)

Enthalpy as well as entropy likes components towards ligand – protein complex binding was analyzed using Prime MMGB-SA (v4.3) approach which includes Generalized-Born/Surface Area continuum solvent model as well as OPLS4 force field¹¹. Calculation of relative binding affinities was done for final XP docked poses keeping VSGB 2.0 solvation model¹³

2.3 Molecular Dynamics

Compound 2542/6R4F complex's extra precision – docked structure was taken for MD simulation with Desmond software of OPLS3e force-field. This was solvated in TIP4P^{14, 15} water and neutralized with 56 sodium ions and 50 counter chloride ions. Now it contains around 63983 atoms and 17825 molecules of water. Again the system was minimized to 25 kcal/mol/Å gradient threshold with OPLS3e force-field of 200 steepest descent and 1000 steps of conjugate gradient. Particle-mesh-Ewald method¹⁶ with a 1e-09 tolerance was used for the electrostatic interactions of long range. Van der Waals and Coulomb interactions were analyzed with cutoff radius of 9 Å. The entire system is placed in 100 ns simulation under an isothermal-isobaric ensemble (NPT) at 300 K temperature and 1 bar pressure. Constant temperature and pressure were maintained throughout the process^{17, 18}. With RESPA integration algorithm the bonded, near nonbonded, and far nonbonded interactions were calculated with time steps of 2, 2, and 6 fs, respectively. 2 fs time step was used for the entire process and data were collected for every 100 ps. Maestro graphical interface was used for the analysis of 3D structures and MD trajectory.

In vitro Studies

2.4 Cytotoxicity Assay¹⁹

L-6 and 3T3 L1 cell lines taken from National Centre for Cell Science, Pune. Cell lines were cultured in DMEM containing 100 IU/ml Penicillin, 10% inactivated fetal bovine serum, 100mg/ml Streptomycin, and 5 mg/ml Amphoterecin-B in 5% CO₂ humid atmosphere at 37 °C. Trypsin (0.2%), EDTA phosphate buffer saline (PBS) solution was used for cell differentiation. Experiments were performed in 96 well microtitre plates and the stock cultures were developed in tissue culture flasks.

Then the cell lines were trypsinized in culture media. 10000 cells/well were plated in 96 well microtitre plate and incubated for 24 h where the monolayer is formed. Control cells were grown with maintenance medium and the drug treated cells were given with different concentration of crude extract. The plates were subjected to incubation at 37 °C with 5% CO₂ for a period of 72 hrs. The changes that occurred in the treatment cells were compared with control cells.

2.5 Sulphorhodamine B (SRB) assay²⁰

50 µL of trichloro acetic acid was added to wells gently and incubated at 4°C for 1 h. The plates were stained with SRB for 30 min. Again the plates were washed for four times with acetic acid to remove the unbound dye. 100 µL of 10 mM tris base was then added to the wells to solubilize the dye. The absorbance was measured using microplate reader at a wavelength of 540 nm and calculated by formula.

$$\% \text{ Growth inhibition} = 100 - \frac{\text{Mean OD of individual test group}}{\text{Mean OD of control}} \times 100$$

2.6 Glucose uptake assay²¹

The cells are cultured and subjected to incubation at 37°C for 48hrs. After the formation of monolayer, the culture was treated with DMEM having 0.2 % Bovine serum albumin (BSA). The culture was again subjected to incubation at 37°C for 18 h. Cells were discarded and washed with KRP buffer after 18h media. The cells were treated with Insulin, Biochanin A and glucose (1M) and incubated at 37°C for 30 min. The Cell lysate was collected for the estimation of glucose. The variation between the glucose content at initial and final stages was recorded by GOD-POD method.

3 Results and Discussion

3.1 In-silico virtual screening, molecular docking and MMGB-SA studies

Analyzing the XP docked poses, the top 10 virtual hits (Table 1) were observed to be form hydrogen bonding, hydrophobic contacts and salt bridges with the linker site residues of 6R4F.pdb (Supplementary Figure 1). The top scored virtual hit compound 2542 (glide g score: -10.09 kcal/mol and MMGB/SA ΔG_{Bind} : -93.01 kcal/mol) (Table 1) formed 7 hydrogen bonds and 1 pi-pi contact with the linker site residues of 6R4F.pdb. In compound 2542, the carbonyl group and hydroxyl group at 3rd and 7th position of chromen-4-one ring formed three hydrogen bonds with Gln310 and Asn465, Gln315 respectively. In the second hit compound 4636 (glide g score: -10.05 kcal/mol and MMGB/SA ΔG_{Bind} : -90.65 kcal/mol), the 4-OH group on the 4-hydroxyphenyl ring at the 2nd position of 2,3-dihydrochromen-4-one ring formed hydrogen

bonding and salt bridge interactions with Asn465, Asp262 and Gln422 with one hydrogen bond. For both the compounds 2542 and 4636, one pi-pi contact was observed between His463 and aromatic ring of 2,3-dihydrochromen-4-one (Figure 1).

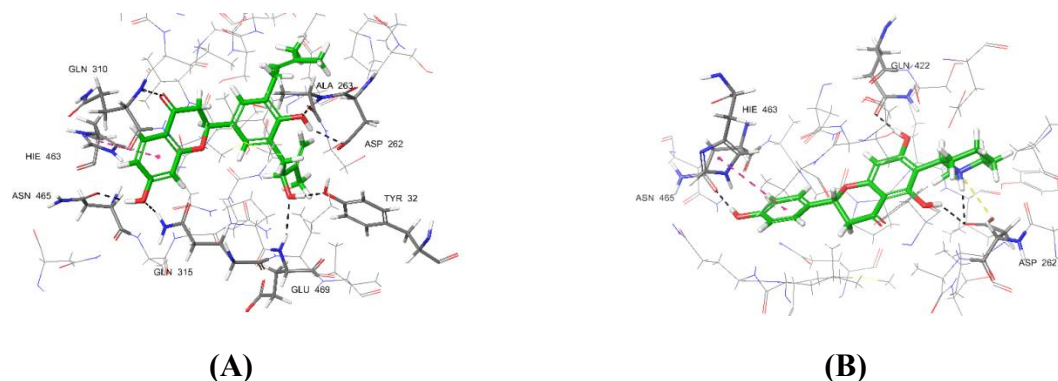


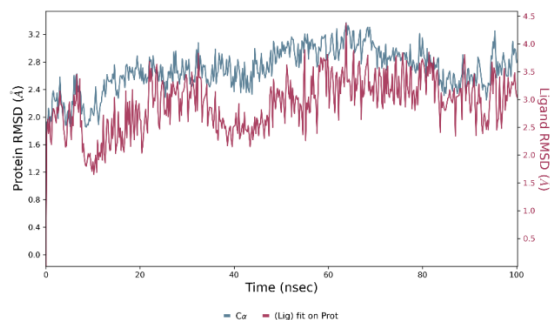
Fig. 1 3D interaction diagram of top score natural compounds (A) 2542 and (B) 4636

S.No	Compound code	Glide gscore	MMGB-SA ΔG_{Bind}	MMGB-SA ΔG_{Coul}	MMGB-SA ΔG_{Hbond}	MMGB-SA ΔG_{Lipo}	MMGB-SA ΔG_{vdW}
1	2542	-10.09	-93.01	21.72	-7.98	-24.50	-10.27
2	4636	-10.05	-90.65	-61.97	-6.78	-25.90	-50.98
3	556	-9.74	-89.50	-26.62	-5.90	-25.87	-52.04
4	12698	-9.58	-88.98	-16.25	-7.27	-22.43	-30.11
5	7064	-9.70	-88.46	-26.30	-7.26	-23.40	-45.20
6	11840	-9.53	-88.08	-101.07	-10.05	-21.72	-35.42
7	9286	-9.63	-83.80	-2.92	-4.32	-26.79	-39.13
8	5827	-9.59	-82.59	-95.25	-10.23	-18.08	-21.62
9	11834	-9.59	-81.00	1.19	-4.87	-19.71	-55.68
10	5829	-9.56	-77.53	-57.52	-10.59	-13.41	-20.91

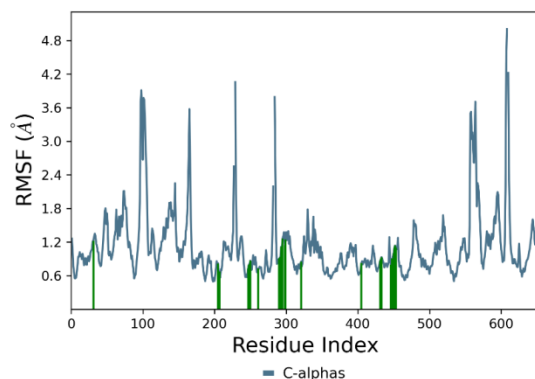
Table 1: XP docking and PRIME MMGB/SA energy values of top scored 10 natural molecules in the catalytic pocket of human GFAT-1 6R4F.pdb

3.2 Molecular dynamics (MD) studies

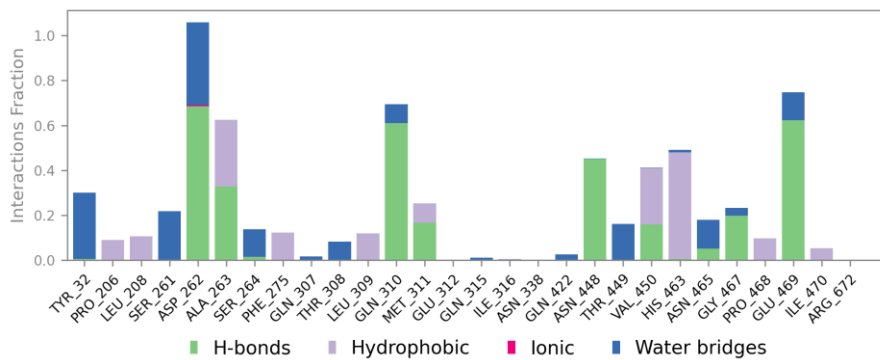
The dynamic behavior of 2542/6R4F.pdb complex was studied by performing a 100ns molecular dynamics simulation. From the simulation trajectory, the RMSD of protein C α atoms was equilibrated for the first 20ns and fluctuated in the range of 2.55 to 3.08 Å (Figure 2A). The ligand RMSD values were observed between 2.45 to 3.8 Å. Protein RMSF values are less than 1.2 Å suggesting the stability of the protein-ligand complex. It was witnessed that amino acid residues Asp262, Ala263, Gln310, Asn448, and Glu469 formed hydrogen bonds with 40-70% of the simulation time and importantly His463 formed hydrophobic pi-pi contacts at 50% of 100ns simulation time. The timeline representation of Protein-Ligand interaction contacts was illustrated in the Figure 3 indicating the stability of compound 2542 throughout the studies.



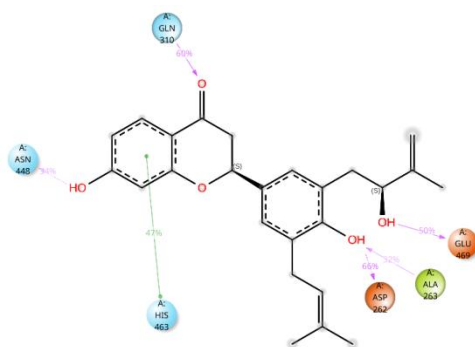
(A)



(B)



(C)



(D)

Fig. 2 (A) RMSD plot (Å) of the simulated positions of Cα atoms of 2542/6R4F.pdb complex during 100ns MD simulation **(B)** Protein RMSF values of 2542/6R4F.pdb complex during 100ns MD simulation **(C)** Bar diagram representing the interactions of inhibitor 2542/6R4F.pdb complex during MD simulation **(D)** 2D trajectory interaction diagram of 2542/6R4F.pdb during 100 ns MD simulation

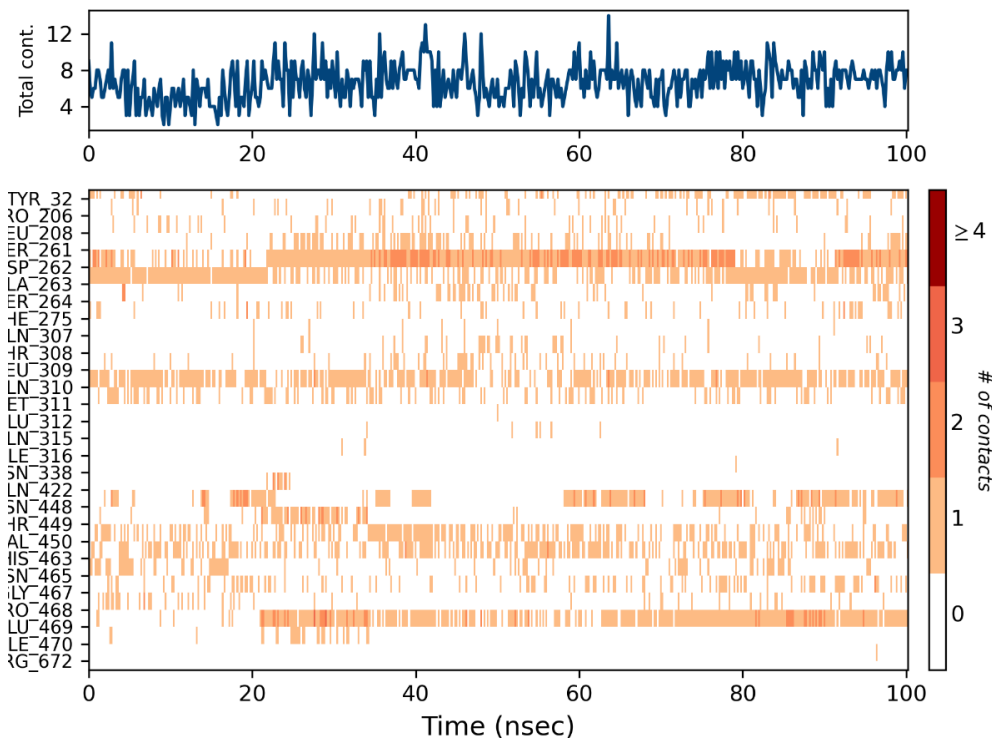


Fig.3 Timeline representation of Protein-Ligand interaction contacts generated from the 100ns simulation trajectory of 2542/6R4F.pdb.

3.3: Cytotoxicity Assay and Sulphorhodamine B (SRB) assay

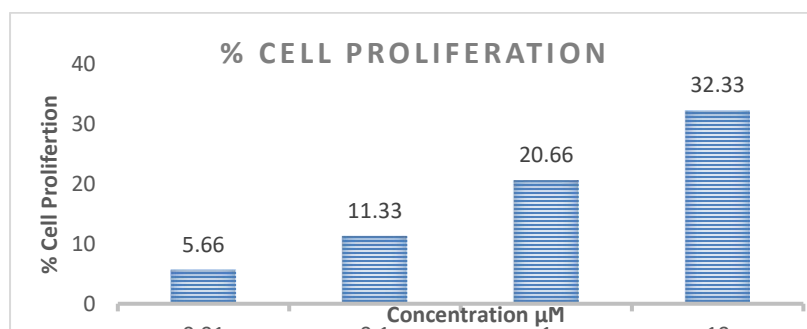


Fig.4 Representation of percentage of cell proliferation

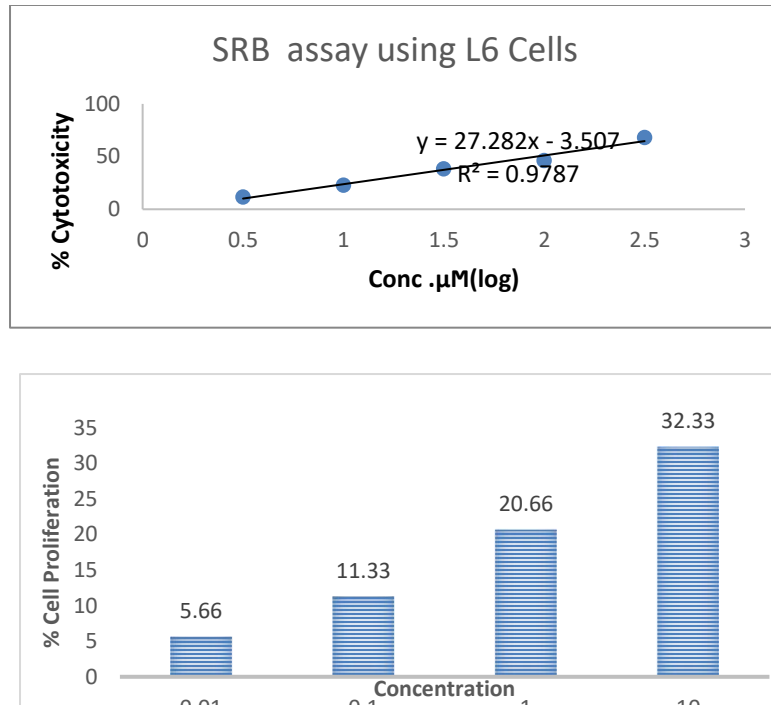


Fig.5 Representation of percentage of cytotoxicity of Biochanin A

Report:

Cytotoxicity assays performed on L-6 and 3T3-L1 cell lines demonstrated IC_{50} values of 50.58 $\mu\text{g}/\text{mL}$ and 35.20 $\mu\text{g}/\text{mL}$, respectively (Figures 4 and 5). These results indicated moderate cytotoxicity of Biochanin A in both cell lines.

3.4 Glucose uptake assay

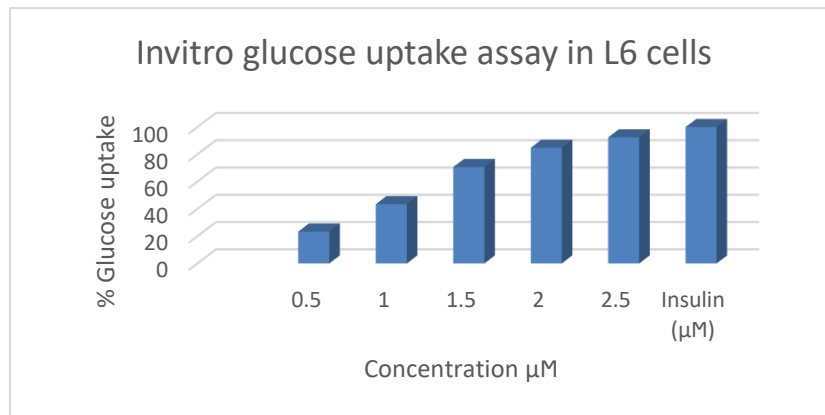
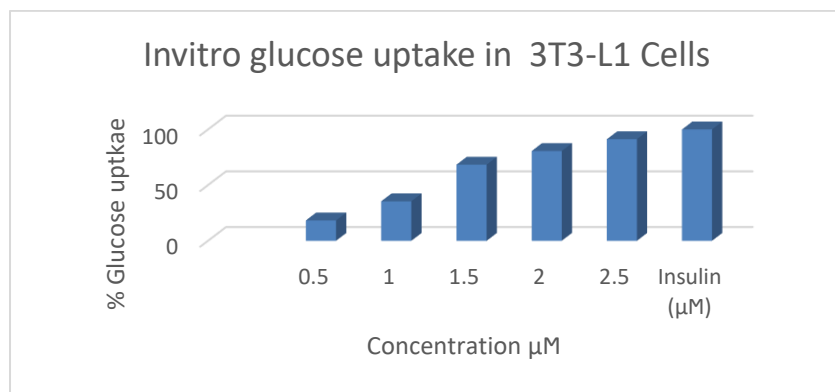


Fig.6 Representation of glucose uptake in L6 cells**Fig.7** Representation of glucose uptake in 3T3-L1 Cells

Report: There was a significant increase in glucose uptake with Biochanin in both cell lines.

4. Conclusion

In conclusion, a high throughput virtual screening was performed employing a COCONUT database comprising of nearly 4 lakh natural compounds. Top 10 virtual hits were chosen in the context of their XP Glide score, binding pocket interactions, and their high negative ΔG_{Bind} scores. Among the top 10 selected hits, compound 2542 exhibited lowest Glide XP score and more negative MMGB/SA binding free energy indicating stronger binding affinity than other hit compounds. Even though, compound 4636 have good glide score, its bonding affinity is much lesser than the compound 2524

In addition to that, **compound 2542** interacted with residues Gln310, Asn448, His463, Asp262, Ala263 and Glu469 suggesting effective stabilization²² whereas hydrogen bond stability of other hit compounds are lesser than the compound 2542. While Asn465 aids in appropriate substrate alignment to guarantee effective isomerization and ammonia transfer, His463 most likely serves as an acid-base catalyst in the isomerase domain²³ Glu469, which is found in the C-terminal tail, is involved in allosteric communication and structural scaffolding. It may also mediate inter-subunit interactions and have an impact on GFAT stability and feedback regulation²⁴. From these studies it was deduced that the binding of these molecules at the linker site may play pronounced modulatory effect inhibiting GFAT enzyme. In-vitro tests demonstrated that the compound has moderate toxicity and glucose

Uptake assay has shown that there is a significant increase in glucose utilization with Biochanin A treatment.

Biochanin A has emerged as a promising drug, having strong binding affinity, structural stability in MD simulations, moderate cytotoxicity, and enhanced glucose uptake activity. These results also support the further development of GFAT-1 inhibitors as novel antidiabetic agents, with possible extensions to antimicrobial therapy. But here it is important to discuss that although the In-silico approaches supported the potentiality of GFAT-1 inhibitors, the enzyme conformational changes may differ with the intracellular environment and long term biological responses. The biological support provided by the in-vitro studies were restricted to cellular models and cannot provide pharmacokinetic and bioavailability results. Hence, it is necessary to proceed for the in-vivo studies to conform the therapeutic efficacy of Biochanin – A

5. References

1. Milewski S. Glucosamine-6-phosphate synthase—the multi-facets enzyme. *Biochim Biophys Acta* [Internet]. 2002;1597(2):173–92. Available from: [http://dx.doi.org/10.1016/s0167-4838\(02\)00318-7](http://dx.doi.org/10.1016/s0167-4838(02)00318-7)
2. Mouilleron, S., Badet-Denisot, M.-A., Badet, B., & Golinelli-Pimpaneau, B. Dynamics of glucosamine-6-phosphate synthase catalysis. *Archives of Biochemistry and Biophysics*, 505(1), 1–12. <https://doi.org/10.1016/j.abb.2010.08.008>
3. Stefaniak J, Nowak MG, Wojciechowski M, Milewski S, Skwarecki AS. Inhibitors of glucosamine-6-phosphate synthase as potential antimicrobials or antidiabetics – synthesis and properties. *J Enzyme Inhib Med Chem* [Internet]. 2022;37(1):1928–56. Available from: <http://dx.doi.org/10.1080/14756366.2022.2096018>
4. Paneque A, Fortus H, Zheng J, Werlen G, Jacinto E. The hexosamine biosynthesis pathway: Regulation and function. *Genes (Basel)* [Internet]. 2023;14(4):933. Available from: <http://dx.doi.org/10.3390/genes14040933>
5. Pompeo F, Byrne D, editors. Uridine diphosphate N-acetylglucosamine orchestrates the interaction of GlmR with either YvcJ or GlmS in *Bacillus subtilis* Elodie Foulquier. In: Anne Galinier *Scientific Reports*. Article Open access Published; 2020. DOI <https://doi.org/10.1038/s41598-020-72854-2>
6. Raczynska, J., Olchowy, J., Konariev, P. V., Svergun, D. I., Milewski, S., & Rypniewski, W. (2007). The crystal and solution studies of glucosamine-6-phosphate synthase from *Candida albicans*. *Journal of Molecular Biology*, 372(3), 672–688. <https://doi.org/10.1016/j.jmb.2007.07.002>
7. Roglic, Gojka. WHO Global report on diabetes: A summary. *International Journal of Noncommunicable Diseases* 1(1):p 3-8, Apr–Jun 2016. | DOI: 10.4103/2468-8827.184853

8. Zimmet, Paul Z et al. Diabetes: a 21st century challenge. *The Lancet Diabetes & Endocrinology*, Volume 2, Issue 1, 56 – 64
9. Lozano, R · Naghavi, M · Foreman, K · et al. Global and regional mortality from 235 causes of death for 20 age groups in 1990 and 2010: a systematic analysis for the Global Burden of Disease Study 2010. *Lancet*. 2012; 380:2095-2128.
10. Frances Gatta. Rebecca Buffum Taylor. Types of Diabetes Mellitus. Medically June 18, 2024.
11. Lu, C., Wu, C., Ghoreishi, D., Chen, W., Wang, L., Damm, W., Ross, G.A., Dahlgren, M.K., Russell, E., Von Bargen, C.D., Abel, R.: OPLS4: improving force field accuracy on challenging regimes of chemical space. *J. Chem. Theory Comput.* 17(7), pp.4291-4300 (2021)
12. Jupudi, S., Azam, M.A., Wadhvani, A.: Design, synthesis and molecular modelling of phenoxyacetohydrazide derivatives as *Staphylococcus aureus* MurD inhibitors. *Chem. Pap.* 75(3), pp.1221-1235 (2021)
13. Li, J., Abel, R., Zhu, K., Cao, Y., Zhao, S., Friesner, R.A.: The VSGB 2.0 model: a next generation energy model for high resolution protein structure modeling. *Proteins: Struct. Funct. Bioinf.* 79(10), pp.2794-2812 (2011)
14. Lawrence, C.P., Skinner, J.L.: Flexible TIP4P model for molecular dynamics simulation of liquid water. *Chem. Phys. Lett.* 372(5-6), pp.842-847 (2003)
15. Jorgensen, W.L., Madura, J.D.: Temperature and size dependence for Monte Carlo simulations of TIP4P water. *Mol. Phys.* 56(6), pp.1381-1392 (1985)
16. Essmann, U., Perera, L., Berkowitz, M.L., Darden, T., Lee, H., Pedersen, L.G.: A smooth particle mesh Ewald method. *J. chem. Phys.* 103(19), pp.8577-8593 (1995).
17. Martyna, G.J., Klein, M.L., Tuckerman, M.: Nosé–Hoover chains: The canonical ensemble via continuous dynamics. *J. Chem. Phys.* 97(4), pp.2635-2643 (1992)
18. Martyna, G.J., Tobias, D.J., Klein, M.L.: Constant pressure molecular dynamics algorithms. *J. chem. Phys.* 101(4177), pp.10-1063. 4177-4189 (1994)
19. Arumugam M, Vijayan P, Raghu C, Ashok G, Dhanaraj SA, Kumarappan CT. Anti-adipogenic activity of *Capsicum annum* (Solanaceae) in 3T3 L1. *J Complem Int Med.* 2008; 5(1): 1-9.
20. Papazisis KT, Geromichalos GD, Dimitriadis KA, Kortsaris AH. Optimization of the sulforhodamine B colorimetric assay. *J Immunol Methods.* 1997; 208: 1518
21. Noipha K, Purintrapiban J, Herunsalee A, Ratanachaiyavong S. *In vitro* glucose uptake activity of *Tinosporacrispa* in skeletal muscle cells. *Asian Biomed.* 2008; 2: 415-20.
22. Ruegenberg, S., Mayr, F.A., Atanassov, I., Baumann, U., Denzel, M.S.: Protein kinase A controls the hexosamine pathway by tuning the feedback inhibition of GFAT-1. *Nat. Commun.* 12(1), p.2176 (2021)
23. Ruegenberg, S., Horn, M., Pichlo, C., Allmeroth, K., Baumann, U., Denzel, M.S.: Loss of GFAT-1 feedback regulation activates the hexosamine pathway that modulates protein homeostasis. *Nat. Commun.* 11(1), p.687 (2020)

24. Paneque, A., Fortus, H., Zheng, J., Werlen, G., Jacinto, E.: The hexosamine biosynthesis pathway: regulation and function. *Genes*. 14(4), p.933 (2023).